https://doi.org/10.47456/bjpe.v10i3.44651 ARTIGO ORIGINAL | OPEN ACCESS

NÚCLEO DE PESQUISA EM GESTÃO DE SISTEMAS DE PRODUÇÃO - NP GSP

Brazilian Journal of Production Engineering
BJPE - Revista Brasileira de Engenharia de Produção
Disponível em: https://periodicos.ufes.br/bjpe

ISSN: 2447-5580

Campus São Mateus
UNIVERSIDADE FEDERAL DO ESPÍRITO SANTO

Pró-Reitoria de Pesquisa e Pós-Graduação
Universidade Federal do Espírito Santo

ANALYSIS OF ENERGETIC AND EXERGETIC PERFORMANCE ACCORDING TO THE EVAPORATION TEMPERATURE OF A VAPOR COMPRESSION CHILLER

ANÁLISE DO DESEMPENHO ENERGÉTICO E EXEGÉTICO DE ACORDO COM A TEMPERATURA DE EVAPORAÇÃO DE UM CHILLER DE COMPRESSÃO DE VAPOR

ANÁLISIS DEL DESEMPEÑO ENERGÉTICO Y EXERGÉTICO SEGÚN LA TEMPERATURA DE EVAPORACIÓN DE UN ENFRIADOR POR COMPRESIÓN DE VAPOR

Carlos Eduardo da Silva Albuquerque [1*], Celso Rosendo Bezerra Filho [2], Thays Nogueira Rodrigues [3], & Maria Deise Calou Leite [4]

[1] Universidade Federal do Vale do São Francisco, Colegiado de Engenharia de produção, Campus Salgueiro-PE
[2] Universidade Federal de Campina Grande, Centro de ciências e tecnologia, Departamento de Engenharia Mecânica
[3 4] Centro Universitário Paraíso, Departamento de Engenharia Civil
[1] carlos.albuquerque@univasf.edu.br [2] celso.rosendo@ufcg.edu.br [3] thays.rodrigues@fapce.edu.br [4] caloudeise@aluno.fapce.edu.br

ARTIGO INFO.

Recebido: 21.05.2024
Aprovado: 05.08.2024
Disponibilizado: 08.08.2024

PALAVRAS-CHAVE: Chiller de compressão de parafuso, Eficiência energética, Eficiência exergética, Temperatura de evaporação

KEYWORDS: Chiller screw compressor, Energy efficiency, Exergy efficiency, Evaporation temperature

PALAVRAS-CHAVE: Chiller com compressor de tornillo, Eficiencia energética, Eficiencia exergética, Temperatura de evaporación

***Autor Correspondente**: **Albuquerque, C. E. da S.**

ABSTRACT

This article presents an energy and exergy efficiency analysis of a large-scale chilled water refrigeration system, a chiller, integrated into a chilled water plant designed to supply the thermal load required for air conditioning in a large shopping mall located in the capital of the state of Paraíba, Brazil. The studied chiller uses a screw-type compressor, which operates with an electric motor to increase the pressure in one phase of the thermodynamic cycle, resulting in significant energy consumption, especially in continuous operations and under high load. The study focuses on reducing electrical energy consumption by evaluating and identifying improvements in the system's operation, based on energy and exergy behavior. To achieve this goal, numerical simulations were performed using the Engineering Equation Solver (EES) software, which allowed the system's operation to be represented and optimized. Additionally, the article presents detailed data on the refrigeration cycle of the studied chiller, essential for understanding the equipment's operation. The results indicate that the evaporator had the highest exergy loss, but this could be reduced by increasing the evaporation temperature, improving the overall efficiency of the refrigeration unit and reducing electrical energy consumption.

RESUMO

Este artigo apresenta uma análise de eficiência energética e exergética de um sistema de refrigeração de água gelada de grande porte, um chiller, integrado a uma central de água gelada projetada para suprir a carga térmica necessária para a refrigeração do ar de um grande shopping localizado na capital do estado da Paraíba, Brasil. O chiller estudado utiliza um compressor do tipo parafuso, que opera com um motor elétrico para aumentar a pressão em uma fase do ciclo termodinâmico, resultando em um consumo significativo de energia, especialmente em operações contínuas e sob carga elevada. O estudo se concentra na redução do consumo de energia elétrica ao avaliar e identificar melhorias na operação do sistema, com base no comportamento energético e exergético. Para alcançar esse objetivo, foram realizadas simulações numéricas utilizando o software Engineering Equation Solver (EES), que permitiram representar e otimizar o funcionamento do sistema. Além disso, o artigo apresenta dados detalhados do ciclo de refrigeração do chiller em estudo, essenciais para compreender o funcionamento do equipamento. Os resultados indicam que o evaporador teve a maior perda de exergia, porém reduzível ao aumentar a temperatura de evaporação, melhorando a eficiência global da unidade de refrigeração e reduzindo o consumo de energia elétrica.

RESUMEN

Este artículo presenta un análisis de eficiencia energética y exergética de un sistema de refrigeración de agua helada de gran tamaño, un chiller, integrado en una central de agua helada diseñada para suplir la carga térmica necesaria para la refrigeración del aire de un gran centro comercial ubicado en la capital del estado de Paraíba, Brasil. El chiller estudiado utiliza un compresor del tipo tornillo, que opera con un motor eléctrico para aumentar la presión en una fase del ciclo termodinámico, resultando en un consumo significativo de energía, especialmente en operaciones continuas y bajo carga elevada. El estudio se concentra en la reducción del consumo de energía eléctrica al evaluar e identificar mejoras en la operación del sistema, basándose en el comportamiento energético y exergético. Para alcanzar este objetivo, se realizaron simulaciones numéricas utilizando el software Engineering Equation Solver (EES), que permitieron representar y optimizar el funcionamiento del sistema. Además, el artículo presenta datos detallados del ciclo de refrigeración del chiller en estudio, esenciales para comprender el funcionamiento del equipo. Los resultados indican que el evaporador tuvo la mayor pérdida de exergía, pero esta se puede reducir aumentando la temperatura de evaporación, mejorando la eficiencia global de la unidad de refrigeración y reduciendo el consumo de energía eléctrica.

INTRODUCTION

In recent years, energy efficiency has emerged as a central concern among engineers and researchers in the field of air conditioning and refrigeration systems. In addition to maintaining environments comfortably cooled, there is a growing need to do so more efficiently, given the significant contribution of these systems to electricity consumption and greenhouse gas emissions (GGE).

Refrigeration and air conditioning systems are responsible for a considerable portion of global electricity consumption (Ismail & Hamdy, 2024). For example, studies indicate that residential air conditioning and refrigeration systems in the United States consume about 28% of household energy (Ruz et al., 2017).

In Brazil, a recent study by the Energy Research Company (EPE) revealed that in 2019, air conditioning systems accounted for 9.4% of national residential electricity consumption (EPE, 2023). Among developing countries in the International Energy Agency (IEA) sample, Brazil has the highest Per Capita Energy Consumption (PCEC) for room cooling. Additionally, the study highlighted a significant 6.9% growth in the consumption of these equipment in the commercial sector in 2022 (EPE, 2023).

The need to improve the energy efficiency of refrigeration systems is not only focused on reducing operational costs but also aligns with global initiatives that promote stricter standards for new constructions, aiming to mitigate GGE emissions associated with electricity generation from fossil fuels (Economidou et al., 2020). It is estimated that the refrigeration and air conditioning sector contribute approximately 1 gigaton of CO_2 equivalent per year (IEA, 2018). Technical studies show that a large part of the energy is lost in air conditioning systems due to energy inefficiencies (Lee et al., 2024).

Various techniques are employed to improve these inefficiencies, including operational data analysis, continuous measurement and monitoring, real-world Testing, and physical laboratory simulations. Among these approaches, optimization of design via numerical simulation can be highlighted. Numerical simulation for the development and optimization of refrigeration systems is a tool that allows, through mathematical models, the prediction of system behavior when subjected to conditions different from the optimal conditions for which they were designed (Lombard et al., 2011; Walker et al., 2014). This method uses a set of equations coded in a computational language and a set of data obtained experimentally. In this way, it is possible to obtain results with a safe margin of error. Numerical simulation is carried out using software that assists in obtaining properties and solving equations. Examples of such software include GateCycle, Aspen Plus, IPSEpro, Cycle-Tempo, and EES (Engineering Equation Solver) (Afram & Janabi-Sharifi, 2014).

Researchers have conducted numerous studies on reducing the energy consumption of refrigeration systems. For instance, Al-qazzaz et al. (2024) compared the use of an underground heat exchanger with a wet cooling tower for cooling purposes, considering technical, economic, and environmental aspects. Conducted in the Mashhad region, where there is a water shortage and high demand for cooling, the energy and water consumption

are calculated and compared through simulation and modeling of both chilled water production methods and the refrigeration cycle. The results show that the underground heat exchanger reduces energy consumption by 14% and eliminates water consumption.

Lyu et al. (2022) investigated the energy and economic performance of magnetic bearing chillers and found energy savings ranging from 10% to 40% compared to traditional centrifugal and scroll chillers. This research suggests that innovations in bearing technology can provide significant improvements in energy efficiency. In line with these findings, Iqbal et al. (2022) conducted exergoeconomic and exergoenvironmental comparative analyses of air conditioning systems using R32 and R410A refrigerants. Their results indicate that R32 offers better energy performance and lower environmental and economic impacts compared to R410A, reinforcing the idea that refrigerant choice plays a crucial role in the energy efficiency of air conditioning systems.

Deymi-Dashtebayaz et al. (2019) complement these findings by optimizing chiller performance under partial load conditions. They achieved an average annual energy saving of 5.6 GWh and a reduction in CO2 emissions by 5.1 tons through adjustments to the number of condenser fans. This optimization highlights the importance of specific operational adjustments to further improve chiller efficiency and sustainability.

Furthermore, Carvalho and de Araujo (2019) expanded the understanding of energy efficiency by evaluating the thermodynamic performance of cascade refrigeration systems using mixed refrigerants. They concluded that refrigerant combinations can provide substantial energy savings and reduce environmental impact, aligning with the need for more sophisticated technological and operational choices to achieve optimal efficiency.

Finally, Jiang et al. (2018) focused on the optimization of injection and inter-stage compression parameters in two-stage compression systems, resulting in a significant improvement in system efficiency and a reduction in energy consumption. Their research complements the view that both technological innovation and operational parameter optimization are essential for enhancing the energy efficiency of air conditioning systems.

In the context of this study, the focus is on the thermodynamic and exergy analysis of a compression chiller, which uses a rotary screw compressor driven by an electric motor. The main disadvantage of this type of chiller, compared to absorption systems, is its high energy consumption. Specifically, the study explores the impact of the evaporation temperature of the refrigerant R134a. Through numerical simulations and thermodynamic analyses, the objective is to identify how adjustments in the evaporation temperature can minimize exergy losses in the main components of the thermodynamic cycle, thereby improving the overall efficiency of the system. This work aims not only to reduce electrical energy consumption but also to contribute to more sustainable practices within the refrigeration sector, addressing significant energy and environmental challenges. Therefore, this study seeks to provide well-founded insights into potential improvements in the operation of water-cooled chillers using screw compressors.

METODOLOGIA

Problem Physical Description

The research aims to evaluate and study, with the aid of numerical simulation, the behavior of energy and exergy efficiencies in relation to variations in the properties of the thermodynamic cycle of a compression chiller. This equipment is among the main components of a Water-Cooled Central (WCC), designed to supply the thermal load necessary for air conditioning in a large shopping mall located in the capital of the state of Paraíba, Brazil. This WCC also includes pumps, cooling towers, valves, and electrical panels

The WCC where the equipment is located is shown in Figure 1. This WCC has 7 chillers, with 6 operating in parallel and 1 as a standby unit, supported by 7 primary pumps and 7 secondary pumps, 7 cooling towers, and an accumulator tank.

Figure 1. External photo of the Water-Cooled Central where the evaluated equipment is integrated

Source: Authors.

In a simplified manner, Figure 2 presents a schematic of this WCC. This WCC operates through a complex system involving several stages and components. The process begins with the six primary pumps (BP), which draw water from the storage tank and direct it to the six chillers in operation. In the chillers, the thermodynamic refrigeration process takes place, utilizing the R134a refrigerant to remove heat from the water circulating through the system. The cooled water, represented by the dark blue lines in Figure 2, returns to the storage tank with the assistance of the secondary pumps (BS).

The second part of the plant is the condensing system, which is equipped with seven cooling towers, one of which is a reserve and six are in operation. The condensing pumps (BC) circulate water from these cooling towers to the chillers, resulting in the condensation of the refrigerant and allowing the thermodynamic cycle to restart within the chillers. The cooling water, represented by the light green lines, circulates through the chillers and, after heating

up during the process, returns to the cooling towers. This water, now represented by the dark green lines, is cooled and prepared to restart the cycle.

Figure 2. Schematic diagram of the WCC where the studied equipment is installed

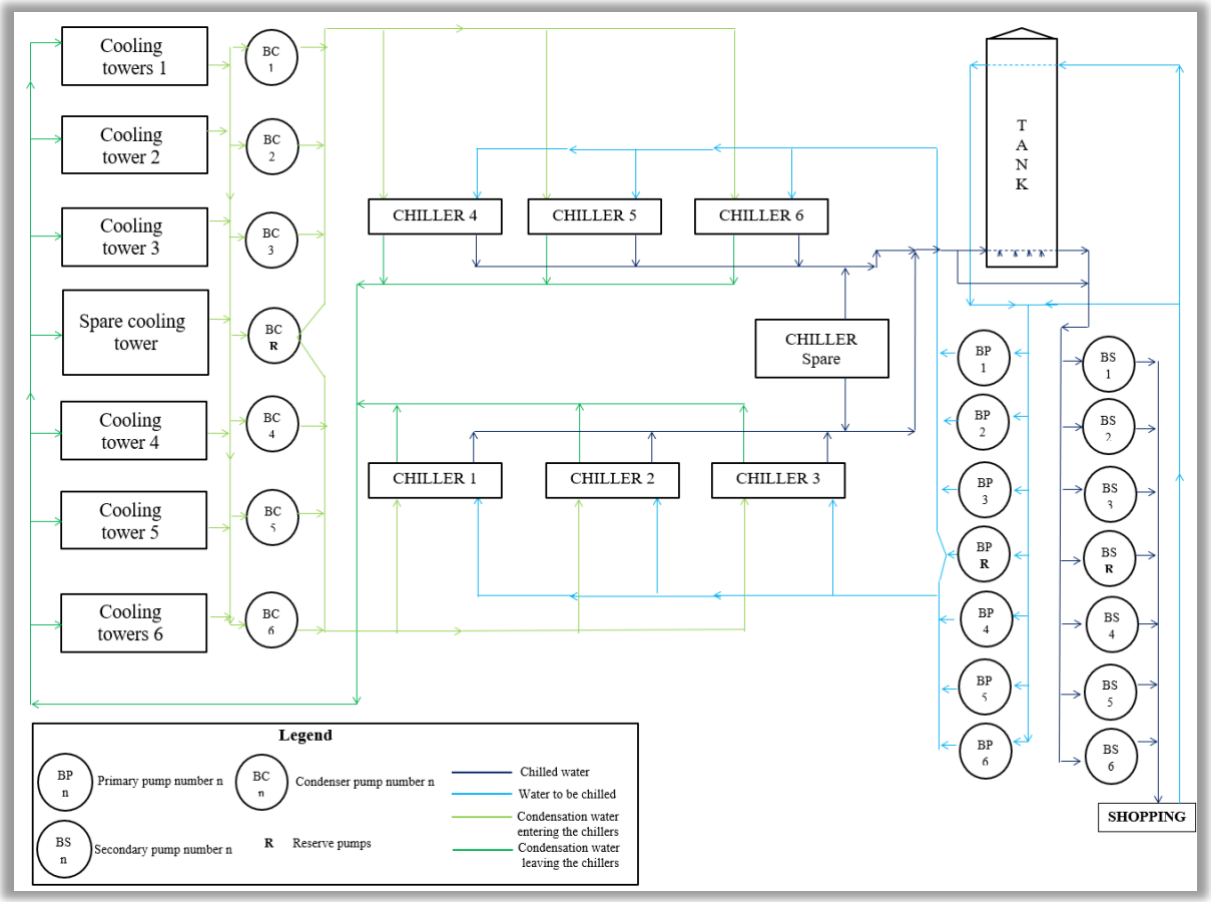

Source: Authors.

The equipment under study is a Carrier chiller model 23XRV with a nominal cooling capacity of 530 TR (1863 kW), operating at 100% capacity. Figure 3 shows a photo of this equipment.

Figure 3. Image of the refrigeration unit used as a model for energy and exergy efficiency study

Source: Authors.

Thermodynamic Cycle

The deficiency of information about any components of the refrigeration cycle was simplified to theoretical model, exclude the cooled of compressor motor and the Direct Frequency Analysis Plate, to enable the development of the research. The cycle studied is showed on the Figure 4.

Due to the lack of information on some components, the refrigeration cycle of the equipment was simplified to enable the development of the study, limiting it to only the standard refrigeration cycle and excluding the cooling of the compressor motor and the VFD (Variable Frequency Drive) plate. The studied cycle is presented in Figure 4.

Figure 4. Schematic representation of the thermodynamic cycle of the evaluated chiller

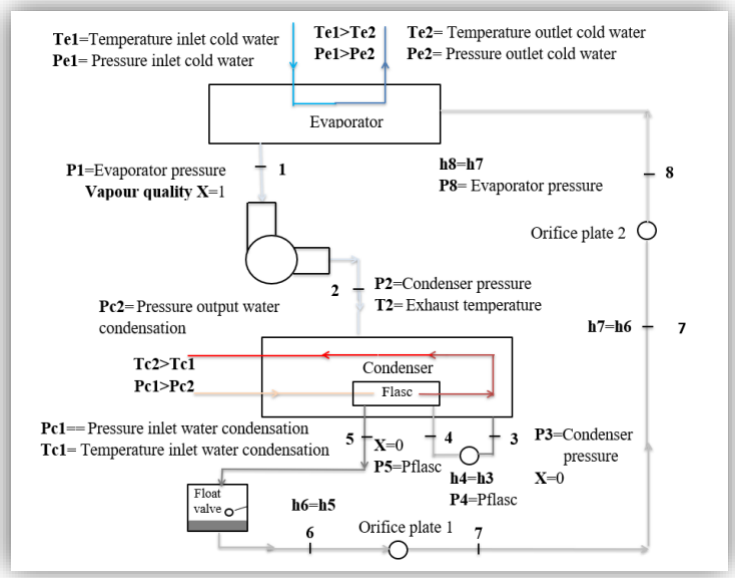

Source: Authors.

The thermodynamic cycle of the equipment has some particularities that need to be defined before its description. The first is that the equipment's condenser includes a FLASC chamber (subcooling chamber), which cools the condensed liquid refrigerant to a reduced temperature, thus increasing the efficiency of the refrigeration cycle. The condensed refrigerant passes through the orifices of the FLASC chamber, where the pressure is lower than that of the condenser. Part of the liquid refrigerant vaporizes, cooling the remaining liquid. The vapor in the FLASC chamber is recondensed in the tubes cooled by the entering condensation water.

Another important component is the float valve, a type of expansion valve that maintains a constant liquid level in a vessel, either directly in the evaporator or in the liquid separators. There are basically two types of float-type expansion valves: the low-pressure float expansion valve and the high-pressure float expansion valve. In this research, the valve used by the evaluated refrigeration unit is the high-pressure type. Its operation, like a well-dimensioned capillary tube, is characterized by keeping the condenser free of liquid and requiring a specific charge of refrigerant to function well. For this, high-pressure float-type expansion valves must be installed at a level lower than the condenser and do not require a liquid receiver (WANG, 2001).

Finally, we have the orifice plates (arranged in series) or float valves, used as throttling devices in centrifugal chillers employing flooded refrigerant feed (WANG, 2001). This device controls the amount of liquid refrigerant fed to the cooler according to the liquid refrigerant pressure in the condenser.

According to Carrier (2008), the thermodynamic cycle of the equipment begins when the compressor (path 1-2 of Figure 4) removes a large volume of gas from the evaporator. When the compressor suction reduces the pressure in the evaporator, the remaining refrigerant starts to boil at a low temperature (280 – 283 K). The energy required for boiling is obtained from the water passing through the evaporator tubes. After absorbing the heat from the water, the refrigerant vapor is compressed. The compression increases the internal energy and enthalpy of the refrigerant fluid, causing its temperature to rise (typically to 305 - 327 K), and it is then discharged from the compressor to the condenser. Cold water passes through the condenser tubes, removing heat from the refrigerant, and the gas liquefies.

The liquid refrigerant passes through the orifices of the FLASC chamber (subcooling). Since the chamber is at low pressure, part of the liquid refrigerant vaporizes, cooling the remaining liquid. The vapor in the FLASC chamber is recondensed in the tubes cooled by the entering condensation water. The liquid drains into the float chamber between the FLASC chamber and the evaporator. Here, the float valve forms a liquid seal, preventing the vapor from the FLASC chamber from entering the evaporator. After passing through the float chamber, the refrigerant is directed to the orifice plates. These devices control the amount of liquid refrigerant fed to the cooler according to the liquid refrigerant pressure in the condenser. During full-load operation, a certain liquid pressure is maintained before the first orifice plate. When the liquid refrigerant flows through the first orifice plate (path 6-7 of Figure 4), there is a pressure drop. However, the fluid pressure between the two orifice plates is still higher than the saturated liquid pressure. Then, at the second orifice plate (path 7-8 of Figure 4), the refrigerant velocity increases again due to the reduction in the orifice plate's section, and the pressure is reduced again to the evaporator pressure, closing the cycle.

To improve the understanding of the presented cycle and enhance clarity in visualizing it, identifying the processes corresponding to the operation of the devices, the Mollier diagram (Pressure x Enthalpy) shown in Figure 5 was created.

Figure 5. Schematic Representation of Mollier Diagram (Pressure vs. Enthalpy) for the Studied Cycle

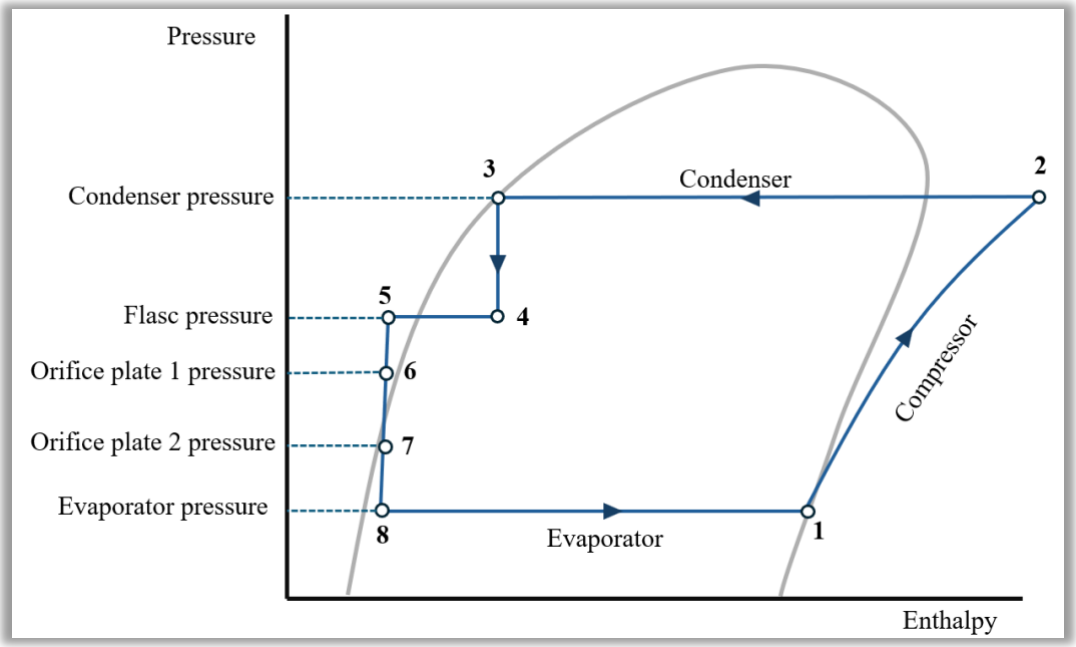

Source: Authors.

The diagram presented in Figure 5 shows that the cycle has three different pressure levels between the condenser pressure (P3) and the evaporator pressure (P8). The first pressure drops between P3 and P4 refers to the reduction from the condenser pressure to the flash tank pressure. The subsequent pressure drops are necessary reductions to control the refrigerant flow according to the equipment's requirements, using orifice plates.

MATHEMATICAL MODELING

To development the mathematical modeling to simulate the operation of the refrigeration cycle, considered: The Chiller is in steady operation, the thermodynamic properties are constant (refrigerant R134a and water) and the fluids flow are uniform in the all section of inlet and outlet and in all the control volume, the heat transfer to the refrigerant from the tube are negligible, the enthalpy of the strangulation process is constant, volumetric flow of the cool and condensation water are constant, the kinetics and potential are negligible and the rate of evaporator pressure, condenser and pipes are negligible too.

The mathematical modeling used had based on the thermodynamic principles. The energetic and exergetic were applied in all components of the thermodynamic cycle.

The Mass Conservation Law applied to Control Volume

The mass conservation law to a control volume affirmed each the mass flow through of the de control surface is the mass rate into the same volume control. The equation 1 is according to Moran et al. (2018) to a mass conservation.

$$\sum \dot{m}_{in} - \sum \dot{m}_{out} = \frac{dm_{cv}}{dt} \quad (1)$$

Where $\dot{m}_{in}$ and $\dot{m}_{out}$ represent the mass flow on the inlet and outlet of the control volume respectively and the $\frac{dm_{cv}}{dt}$ is the mass rate in the control volume, which is equal to 0 for steady state.

The Energy Conservation Law applied to Control Volume

The energy conservation law had known like the first law of thermodynamic. This law is the amount energy and ensure that energy cannot be created or loser, only transformed. To a control volume, it is expressed according to Moran et al. (2018) in the equation 2.

$$\frac{dE_{cv}}{dt} = \dot{Q}_{CV} - \dot{W}_{cv} + \sum \dot{m}_{in}\left(h_{in} + \frac{V_{in}^2}{2} + gz_{in}\right) - \sum \dot{m}_{out}\left(h_{out} + \frac{V_{out}^2}{2} + gz_{out}\right) \quad (2)$$

Where the first term located in the left side, $\frac{dE_{cv}}{dt}$, is the rate of energy into the control volume which is equal to 0 for steady-state, and the other term located in the right side are: $\dot{Q}_{CV}$ the rate of heat transfer, $\dot{W}_{cv}$ work, $\sum \dot{m}_{in}\left(h_{in} + \frac{V_{in}^2}{2} + gz_{in}\right)$ e $\sum \dot{m}_{out}\left(h_{out} + \frac{V_{out}^2}{2} + gz_{out}\right)$ energy in the inlet and outlet respectively, where the *h* is the enthalpy, *V²/2* is the kinetic energy and gz, is the potential energy, all of them per unit of mass.

The Second Law of Thermodynamic

The first law of thermodynamic quantify the energy, while the second law show each the energy have quality and the processes ever occur in the way of energy degradation. It can be express mathematically using the entropy. The expression of the second law to a control volume according to Moran et al. (2018) had represents in the equation 3.

$$\frac{dS_{cv}}{dt} = \sum\left(\frac{\dot{Q}_{cv}}{T}\right) + \sum \dot{m}_{in}s_{in} - \sum \dot{m}_{out}s_{out} + \dot{\sigma}_{ger} \quad (3)$$

Where $\frac{dS_{cv}}{dt}$ represents the rate of entropy into the control volume which is equal to 0 for steady-state, $\sum\left(\frac{\dot{Q}_{cv}}{T}\right)$ the totally heat transfer from the system, $\sum \dot{m}_{in}s_{in} - \sum \dot{m}_{out}s_{out}$ the balance of entropy (inlet and outlet) in the control volume by the mass flow through the control surface and $\dot{\sigma}_{ger}$ the entropy generation, that is empty to the reversible and positive to irreversible processes.

Exergetic Balance

The exergetic balance had define as the maximum theoretical work for a system, when it, in the stage, interacts with the main to get the thermodynamic equilibrium Moran et al. (2018). Torío (2009) defined exergy like a measure of the potential energy flux, it can be change in the high-quality energy. The balance of the exergy to a rate of control volume according Çengel & Boles (2015) had represented by the equation 4.

$$\frac{dX_{cv}}{dt} = \sum_j \left(1 - \frac{T_0}{T}\right)\dot{Q}_J - \left(\dot{W}_{cv} - p_0\frac{d\forall}{dt}\right) + \sum_{in} \dot{m}x_{fin} - \sum_{out} \dot{m}x_{fout} - \dot{X}_L \quad (4)$$

Where the first term on the left, $\frac{dX_{cv}}{dt}$, is the rate of change of exergy over time within the control volume, the terms on the right are respectively $\sum_j \left(1 - \frac{T_0}{T}\right)\dot{Q}_J$ the rate of exergy transfer associated with heat transfer to the control volume at a boundary region where the temperature is T, $\left(\dot{W}_{cv} - p_0\frac{d\forall}{dt}\right)$ the control volume work associated to the rate of exergy,

$\sum_{in} \dot{m}x_{fin} - \sum_{out} \dot{m}x_{fout}$ the totally exergy from the flux of mass into the control volume (inlet and outlet) and $\dot{X}_L$ the rate of exergy destruction associated with irreversibility within the control volume.

Energetic and Exergetic efficiecy

The energetic efficiecy to a refrigeration cycle had represented by the COP (Coefficient Operation Performance) as equation 5.

$$COP = \frac{\text{Heat removed from the hot environment}}{Work\ done} = \frac{\dot{Q}_{refrigeration}}{W_{liquid}} \quad (5)$$

The term $\dot{Q}_{refrigeration}$ represents the thermal load removed from the environment to be refrigerated, andW_{liquid} represents the work done.

The exergetic efficiecy, η_{II}, is defined as:

$$\eta_{II} = \frac{\text{Exergy recovered}}{\text{Exergy provided}} = 1 - \frac{\text{Exergy loss}}{\text{Exergy provided}} \quad (6)$$

Exergy recovered refers to the amount of exergy that is recuperated from a process or system, representing the usable energy portion capable of being converted into work. Exergy provided denotes the total exergy introduced into a system, originating from sources like heat, work, or mass flow with specific exergy content. Exergy loss quantifies the exergy that is irreversibly destroyed during the process, attributable to factors such as friction, heat dissipation, or non-ideal mixing. This exergy cannot be recovered to perform useful work. Exergy supplied, like exergy provided, encompasses the total exergy inputted into the system, encompassing all sources of exergy

MODELING EVALUATION

As mentioned earlier, the device under study is in operation at a large commercial facility for chilled water production. This facility has a monitoring center where information and data on its operation under stable conditions were obtained. The device was modeled using Engineering Equation Solver (EES), a widely used software among engineers to solve engineering problems, especially in the areas of fluid mechanics, heat transfer, and thermodynamics. It allows users to perform detailed analyses and numerical simulations using an extensive library of thermodynamic properties. In the case of the model created in this research, the thermodynamic properties of the refrigerant R134a were obtained from this software's library.

After modeling the standard behavior of the equipment and validating it through comparisons with operation data provided by the manufacturer and the engineer responsible for the facility, it was possible to simulate the equipment's behavior under other operational conditions. This result was used to validate the numerical model.

The data from the steady-state operation of the studied chiller operating at 92% of its capacity are detailed in Table 1.

Table 1. Steady-State Operation Data of the Studied Chiller

Proprieties	Inlet	Outlet
Environment temperature (°C)	28.00	
Evaporator pressure (kPa)	265.00	265.00
Condenser pressure (kPa)	830.00	830.00
Temperature of the refrigerant condenser (°C)	37.30	-
Temperature of the water evaporator (°C)	15.60	6.50
Temperature of the water condenser (°C)	30.60	35.60
Pressure of the water evaporator (kPa)	382.00	333.00
Pressure of the water condenser (kPa)	156.90	107.87
Mass flux of water into condenser (kg/s)	94.40	
Mass flux of water into evaporator (kg/s)	44.70	
Consume of the compressor motor (kW)	272.00	

Source: Authors.

RESULTS AND DISCUSSIONS

Validation of the mathematical model

The validation and reliability assessment of the mathematical model were conducted by comparing the simulation results with the information collected at the chiller monitoring center in the WCC.

These data, previously shown in Table 1, were obtained under stable operating conditions with 92% working capacity. The results were compared with the data collected by the engineer responsible for the refrigeration unit, which showed a working capacity of 87%, as well as with the manual data, which assumes 100% operational capacity of the equipment, and with literature data, the latter focusing mainly on exergy data.

Table 2 shows the comparison of the results obtained through simulations with the manufacturer's data and the data calculated by the establishment's responsible party.

The cooling capacity obtained from the simulation was 1,705.00 kW, approximately 485.13 tons of refrigeration (TR). According to the equipment manual, at 100% working capacity, the cooling capacity is 530.00 TR, approximately 1,863.00 kW. Additionally, the work obtained in the simulation was 265.10 kW, while the electric motor of the compressor consumed 272.00 kW on the day of measurement. Knowing that the efficiency of the motor-compressor unit is approximately 96%, the compressor work would be 261.12 kW, a value close to the simulation result (Carrier, 2008).

Table 2. Comparison of simulation results with manufacturer and calculated data

Datas	Simulation	Manufacturer date	Datas Equipament	Cavalcante & Moreira (2016)	
Compressor work (kW)	265.10	292.00	259.00	-	-
Isentropic compressor work (kW)	206.80	-	-	-	-
Cooling capacity (kW)	1,705.00	1,863.00	1,663.54	-	-
Heat rejection rate (kW)	1,970.00	-	-	-	-
COP (-)	6.43	6.39	6.42	6.04	5.22
Reversible COP (-)	6.54	-	-	-	-
Exergy efficiency of the cycle (%)	42.80	-	-	41.28	47.78
Exergy efficiency of the evaporator (%)	51.17	-	-	68.20	68.06
Exergy efficiency of the compressor (%)	98.43	-	-	86.46	85.70
Exergy efficiency of the condenser (%)	92.45	-	-	0.00	0.00

Source: Authors and Cavalcante & Moreira (2016)

The difference between the simulation values and the manufacturer's data is primarily attributed to operational conditions and secondly to simplifications made in the modeling. The value closest to the simulation is that of the equipment data, suggesting that the simulation may be well adjusted to real conditions, albeit in a slightly different operating range.

A comparative analysis, from the aspect energetic and exergetic, between two unities of compression refrigeration of steam into a shopping from Teresina-PI was presented by Cavalcante (2016), where was analyzed two models of Chiller, YSEAEAS4-CP and YKECERQ7-EPG.

The equipment's availed for Cavalcante (2016) had been refrigeration capacity and work conditions similar to equipment studied on this research. Analyzing the result's presented on the Table 2, can be confirm the values of COP and exergetic efficient of the cycle and every component resembles proportionally. Occur a divergence in the condenser because the considerations about the temperature of the hot source and the environment were considered equals by Cavalcante (2016), different of the considered in this research.

Iqbal et al. (2022) and Li et al. (2020) found in their studies that high rates of exergy destruction typically concentrate in the evaporator and condenser, while remaining below 10% in other components. A similar case was observed in the model presented in this research, differing only in the condenser, where lower exergy destruction was noted due to the Flasc chamber (undercooling). Figure 6 depicts the percentage of exergy destruction obtained in this case for all the main elements studied in this research.

Figure 6. Exergy losses for the main systems elements

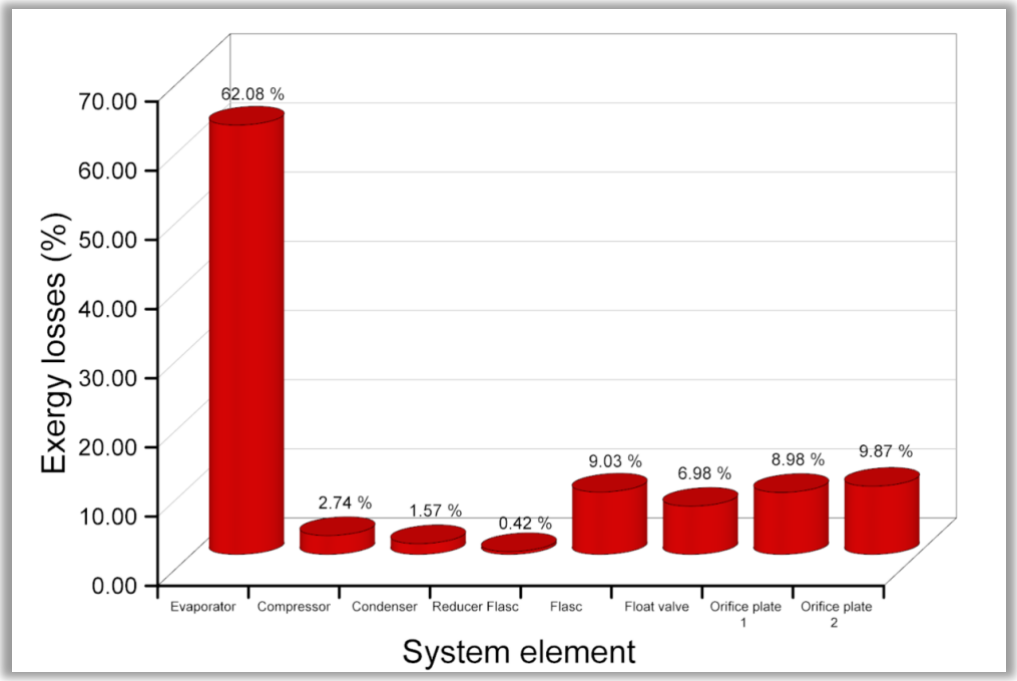

Source: Authors

Range of the evaporation temperature

The results presented in this section are associated with the change in the refrigerant's evaporation temperature in state 1, where, according to the simulation analysis under normal operating conditions, the value presented was -2.74 ºC.

Table 3 shows the COP values obtained with the variation of the evaporation temperature. It is important to note that the temperature values presented are imposed as input conditions in the model, and the results obtained are the outcome of numerical simulations.

Table 3. COP's obtained as function of the evaporation temperature

Evaporation temperature (°C)	COP (-)	Evaporation temperature (°C)	COP (-)
-5.00	5.65	0.26	6,56
-4.47	5.73	0.79	6,67
-3.95	5.81	1.32	6,77
-3.42	5.90	1.84	6,88
-2.90	5.99	2.37	6,99
-2.37	6.08	2.90	7,11
-1.84	6.17	3.42	7,23
-1.32	6.26	3.95	7,35
-0.79	6.36	4.47	7,48
-0.26	6.46	5.00	7.61

Source: Authors.

When analyzing the data presented in Table 3, it is observed that the COP of the equipment increases as the evaporation temperature of the refrigerant in state 1 rises. Studies by Massuvhetto et al. (2019), Qin et al. (2021), and Rodriguez Jara et al. (2022) reported similar behavior, where the condensation temperature remains constant while the saturation temperature in the evaporator increases, reflecting an efficiency increase predicted by the Carnot cycle.

Thermodynamically, the increase in COP shown in this work and in other studies is explained by the reduction in the temperature difference between the evaporator and the condenser when the evaporation temperature increases. This reduces the work done by the compressor to transfer heat from the evaporator to the condenser, improving the cycle's efficiency and resulting in a higher COP (Çengel & Boles, 2015).

Additionally, Figure 7a shows that the increase in evaporation temperature directly influences the evaporation pressure and reduces the pressure delta between the condenser and the evaporator, which consequently decreases the compressor's electrical energy demand, as shown in Figure 7b.

Figure 7. Effect of the range of the evaporation temperature a) pressure of the state 1; b) Work consumed by the compressor

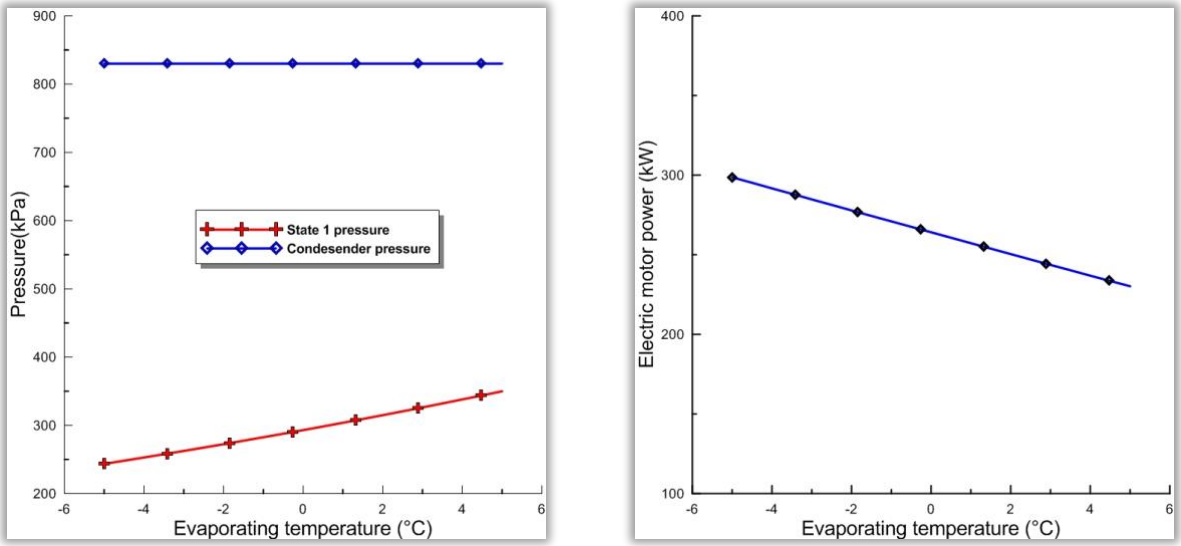

(a) (b)

Source: Authors.

However, it is important to note that the presented data are theoretical assumptions based on simulated numerical results. In practice, this increase in COP is limited by several factors. For instance, compressors may have reduced efficiency or face operational issues at higher evaporation temperatures. Each refrigerant has an ideal performance limit; beyond this point, increasing the temperature can result in lower efficiency. Additionally, the efficiency of heat exchangers may decrease, limiting the effectiveness of heat transfer.

Figure 8 illustrates the exergetic efficiency behavior for each of the main components investigated in this study.

Figure 8. Exergetic efficiency of the main componets as function the evaporation temperature

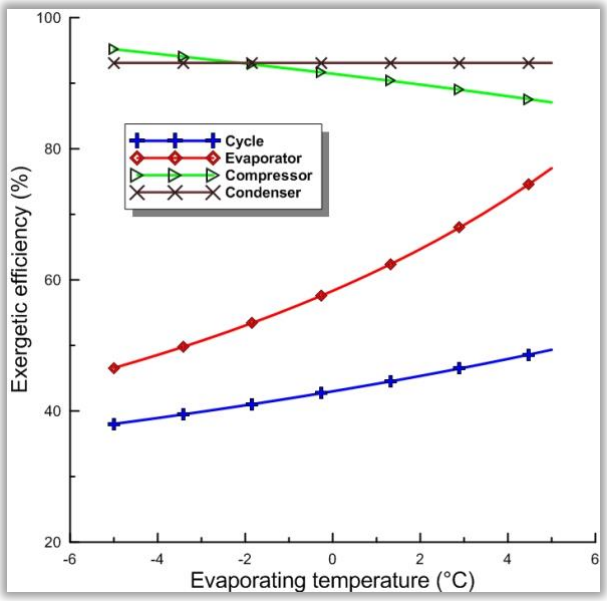

Source: Authors.

Upon analyzing these curves, it becomes evident that the exergetic efficiency of the evaporator experienced a significant increase of approximately 30.47% within the temperature range of -5 to 5 ºC. This increase reflects a reduction in exergy destruction within the evaporator, as at -5 ºC, approximately 61.15% of the total exergy losses of the system are attributed to this component, decreasing to 25.22% at 5 ºC. In contrast, the compressor exergy losses represent 25.23% in the worst-case scenario.

This result indicates that optimizing the operational conditions or the design of the evaporator can lead to significant improvements in the overall efficiency of the system by minimizing exergy losses in this critical component.

Additionally, an inverse behavior in the exergetic efficiency of the cycle was observed, where the compressor demonstrated a reduction in its exergetic efficiency. This observation underscores the importance of considering not only each component individually but also their interactions to fully understand the exergetic efficiency of the system as a whole.

The comparative analysis between the exergy losses in the evaporator and the compressor highlights that losses in the evaporator exert a substantially greater influence on the overall performance of the system. This phenomenon, clearly visible in Figure 9, corroborates previous findings by Jiang et al. (2018), Rad and Maddah (2019), and Wei et al. (2020) also demonstrate in their studies that an increase in evaporation temperature leads to a rise in COP and exergy efficiency, while the total irreversibility rate decreases.

Figura 9. Exergy losses of the main components as function of the evaporation temperature

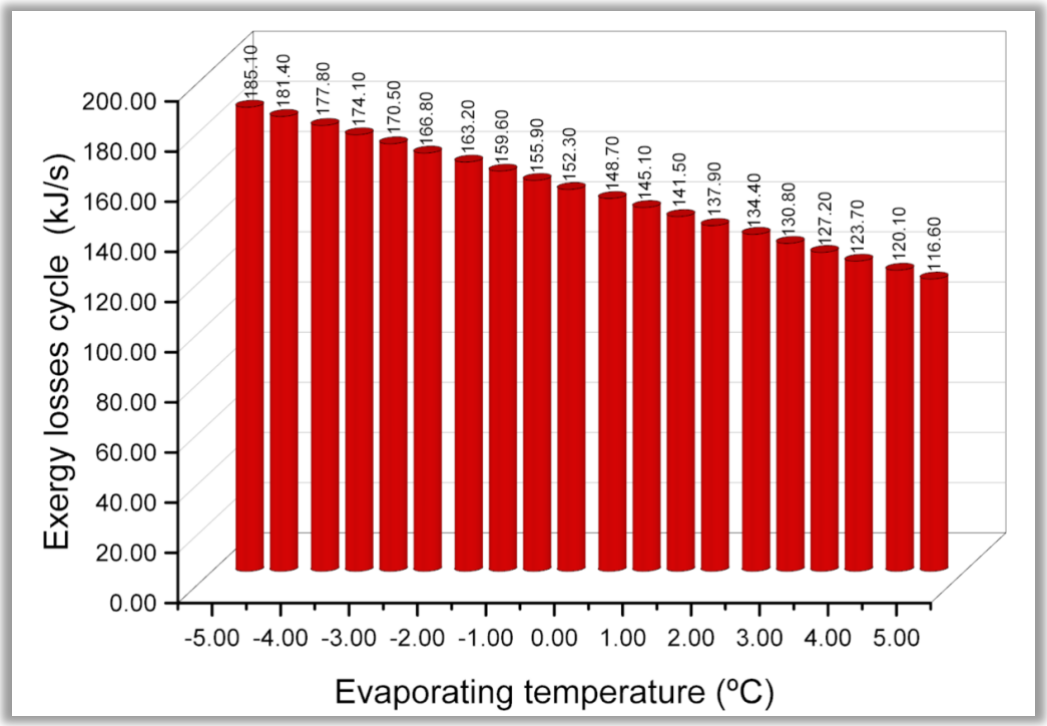

Source: Authors.

CONCLUSIONS

In this work, the cooling of a compression chiller cycle that uses a screw compressor, varying the work equipment evaporation temperatures within an acceptable range, considering the particularities cycle developed by equipment and destructions exergy. It can be concluded after analysis of the results that:

✓ At a constant condensing temperature (constant pressure in the condenser), the COP of the machine, based on the shaft power, increased with the increase of the saturation temperature in the evaporator, showing a behavior like a Carnot refrigerator.

✓ Higher values of efficiency for the 1st and 2nd laws of thermodynamics occur due to the approach of condenser pressure to evaporator pressure caused by the increase in simulated evaporation temperature. This pressure approach causes a reduction in the work consumed by the equipment, thus generating an increase in efficiency.

✓ The exergetic efficiency of the evaporator shows a considerable increase of approximately 30.47% in the temperature range from -5 to 5 °C.

✓ There is an increase in the exergy efficiency of the cycle, even if the compressor showed a reduction in its exergy efficiency.

✓ The reduction of exergy destruction in the evaporator has a greater influence on the system efficiency than the exergy destruct.

✓ The reduction of exergy losses in the evaporator emerges as a crucial strategic target to improve the overall exergetic efficiency of the system, highlighting the importance of strategies aimed at mitigating irreversibility in this specific component to optimize overall energy performance.

REFERÊNCIAS

Afram, A. & Janabi-Sharifi, F. (2014). Theory and applications of HVAC control systems – A review of model predictive control (MPC). *Building and Environment*, 72, 343-355. https://doi.org/10.1016/j.buildenv.2013.11.016

Al-Qazzaz, A. H. S., Farzaneh-Gord, M., & Niazmand, H. (2024). Energy and exergy analysis with environment benefit of the underground cooling system of the chiller plant. *Results in Engineering*, 22, 101952. https://doi.org/10.1016/j.rineng.2024.101952

Carrier. (2008, julho). *Manual de instalação, operação e manutenção Chiller* EVERGREEN 23XRV. Recuperado de http://www.carrierdobrasil.com.br/modelo/downloads/meu-negocio/32/aquaedge-23xrv

Cavalcante, A. M. C. C., & Moreira, H. L. (2016). Análise exergética comparativa entre duas unidades de refrigeração por compressão de vapor de um shopping center localizado em Teresina-PI. Artigo publicado no CONEM. https://doi.org/10.20906/CPS%2FCON-2016-0930

CEEETA, Centro de Estudos em Economia da Energia, dos Transportes e do Ambiente. (2001, dezembro). *Tecnologias de micro-geração e sistemas periféricos. Parte II – Tecnologias de aproveitamento de calor*.

Çengel, Y. A., & Boles , M. A. (2013). *Termodinâmica* (8ª ed.). Porto Alegre: McGraw-Hill Education.

Chumioque, J. J. R. (2004). Simulação de um sistema de refrigeração com termoacumulação operando em regime transiente (Dissertação de mestrado). *Pontifícia Universidade Católica do Rio de Janeiro*, Departamento de Engenharia Mecânica.

Deymi-Dashtebayaz, M., Farahnak, M., Nazeri Boori Abadi, R., (2019). Energy saving and environmental impact of optimizing the number of condenser fans in centrifugal chillers under partial load operation. *International Journal of Refrigeration*, 103, 163-179. https://doi.org/10.1016/j.ijrefrig.2019.03.020

Economidou, M., Todeschi, V., Bertoldi, P., D'Agostino, D., Zangheri, P., & Castellazzi, L. (2020). Review of 50 years of EU energy efficiency policies for buildings. Energy and Buildings, 225. https://doi.org/10.1016/j.enbuild.2020.110322

EPE, Empresa de Pesquisa Energética. (2023). *Atlas da Eficiência Energética Brasil 2023*. Recuperado de https://www.epe.gov.br/sites-pt/publicacoes-dados-abertos/publicacoes/PublicacoesArquivos/publicacao-788/Atlas%20da%20Efici%C3%AAncia%20Energ%C3%A9tica%20Brasil%202023.pdf

Ismail, M. & Hamdy, H. (2024). Influence of coupling air conditioner with hybrid PCMs on building interior conditions and consumed power: Experimental investigation. *Energy and Buildings*, 310, 114112.

https://doi.org/10.1016/j.enbuild.2024.114112
International Energy Agency (IEA). (2018). *The Future of Cooling: Opportunities for energy-efficient air conditioning*. IEA Publications. Website:https://www.iea.org/reports/the-future-of-cooling
Iqbal, M. T., Tariq, A., Anis, A., & Ahn, J. (2022). Comparative exergoeconomic and exergoenvironmental analyses of two air conditioning systems using R32 and R410A refrigerants. *Energy Conversion and Management*, 255, 114415. https://doi.org/10.1016/j.enconman.2022.114415
Jiang, S., Wang, S. G., & Jin, X. (2018). Numerical research on coupling performance of inter-stage parameters for two-stage compression system with injection. *Applied Thermal Engineering*. https://doi.org/10.1016/j.applthermaleng.2017.09.126
Li, X., Zhang, Y., Zhang, X., & Wang, R. (2020). Exergy analysis and optimization of a CO2 transcritical refrigeration system with parallel compression and ejector expansion. Energy, 210, 118545. https://doi.org/10.1016/j.energy.2020.118545
Lombard, L. P., Ortiz, J., & Maestre, I. R. (2011). The map of energy flow in HVAC systems. *Applied Energy*, 88(12), 5024-5031
https://doi.org/10.1016/j.apenergy.2011.07.003
Lyu, W., Wang, Z., Li, X., Xin, X., Chen, S., Yang, Y., Xu, Z., Yang, Q., Li, H. (2022). Energy efficiency and economic analysis of utilizing magnetic bearing chillers for the cooling of data centers. *Journal of Building Engineering*, 48, 103920. https://doi.org/10.1016/j.jobe.2021.103920
Mahdi, D.-D., Mehdi, F., & Reza, N. B. A. (2019). Energy saving and environmental impact of optimizing the number of condenser fans in centrifugal chillers under partial load operation. *International Journal of Refrigeration*, 103, 163-179. https://doi.org/10.1016/j.ijrefrig.2019.03.020
Massuchetto, L.H.P., do Nascimento, R.B.C., de Carvalho, S.M.R., de Araujo, H.V. (2019). Thermodynamic performance evaluation of a cascade refrigeration system with mixed refrigerants: R744/R1270, R744/R717, and R744/RE170. *International Journal of Refrigeration,* 106, 201-212. https://doi.org/10.1016/j.ijrefrig.2019.07.005
Moran, M. J., Shapiro, H. N., Boettner, D. D., & Bailey, M. B. (2018). Princípios de termodinâmica para engenharia. LTC.
Qin, Y., Li, N., Zhang, H., & Liu, B. (2021). Thermodynamic performance of a modified −150 °C refrigeration system coupled with Linde-Hampson and three-stage auto-cascade using low-GWP refrigerants. *Energy Conversion and Management,* 236, 114093.
https://doi.org/10.1016/j.enconman.2021.114093
Rad, E. A., & Maddah, S. (2019). Entropic optimization of the economizer's pressure in a heat pump cycle integrated with a flash-tank and vapor-injection system. *International Journal of Refrigeration*. https://doi.org/10.1016/j.ijrefrig.2018.09.018
Rodriguez-Jara, E.A., Sanchez-de-la-Flor, F.J., Expósito-Carrillo, J.A., & Salmeron-Lissen, J.M. (2022). Thermodynamic analysis of auto-cascade refrigeration cycles, with and without ejector, for ultra low temperature freezing using a mixture of refrigerants R600a and R1150. *Applied Thermal Engineering, 200*, 117598.
https://doi.org/10.1016/j.applthermaleng.2021.117598
Ruz, M. L., Garrido, J., Vázquez, F., & Morilla, F. (2017). A hybrid modeling approach for steady-state optimal operation of vapor compression refrigeration cycles. *Applied Thermal Engineering*, 120, 74-87. https://doi.org/10.1016/j.applthermaleng.2017.03.103
Sathtasivam, J., Tang, G., & Ng, K. C. (2010). Evaluation of the simple thermodynamic model (Gordon and Ng universal chiller model) as a fault detection and diagnosis tool for on-site centrifugal chillers. International *Journal of Air-Conditioning and Refrigeration.*
https://doi.org/10.1142/S2010132510000071
Torío, H., Angelotti, A., & Schmidt, D. (2009). Exergy analysis of renewable energy-based climatisation systems for buildings: A critical view. *Energy and Buildings*, 41. https://doi.org/10.1016/j.enbuild.2008.10.006
Walker, G., Shove, E., & Brown, S. (2014). How does air conditioning become 'needed'? A case study of routes rationales and dynamics. *Energy Research & Social Science*, 4, 1-9.
https://doi.org/10.1016/j.erss.2014.08.002
Wang, S. K. (2001). *Handbook of air conditioning and refrigeration* (2ª ed.). Editora McGraw-Hill.
Wei, W. Z., Ni, L., Zhou, C. H., Yao, Y., Xu, L. F., & Yang, Y. H. (2020). Performance analysis of a quasi-two stage compression air source heat pump in severe cold region with a new control strategy. *Applied Thermal Engineering*.
https://doi.org/10.1016/j.applthermaleng.2020.115317
Yang, L. & Yuan, X. (2013). A numerical study on the performance of a ground-coupled heat pump system in a hot and humid area. Energy and Buildings, 65, 101-110. https://doi.org/10.1016/j.enbuild.2013.06.018